·综述·

一体化快堆燃料包壳用铁素体/马氏体钢研究进展

冯 伟[1]，关淞元[2,3]，李峻宏[1]，单鹏展[2,3]，邢炜伟[2,3]，郝宪朝[2,3]，梁 田[2,3]，马颖澈[2,3]
（1 中国原子能科学研究院，北京 102413；2 中国科学院金属研究所师昌绪先进材料创新中心，沈阳 110016；
3 中国科学院核用材料安全与评价重点实验室，沈阳 110016）

摘 要：一体化快堆采用金属燃料，燃料包壳工作温度介于350~630 ℃，工作周期将最长达到50 000 h以上。随着工作周期延长，包壳承受的快中子辐照剂量将由目前的MOX燃料的80 dpa增加到150~300 dpa，因此，发展承温能力高、抗辐照性能优异的新型包壳材料，成为一体化快堆发展的重要组成部分。文章概述了铁素体/马氏体钢（铁马钢）材料的发展背景，分析了不同牌号铁马钢力学性能、辐照性能特点及不同合金元素对钢的性能的影响规律，进而提出了适用于一体化快堆堆芯组件用铁马钢材料的合金优化策略。利用优化策略对HT9钢进行初步改进，改进后的HT9G进行室温拉伸测试和700 ℃/100 MPa持久寿命测试。结果表明，改进后的合金具有良好的拉伸强度和持久寿命，其室温屈服强度可达880 MPa，比T91钢提高约310 MPa，比HT9和T92钢提高约80~120 MPa；700 ℃、100 MPa持久寿命达372~385 h，远高于HT9同条件下的70~82 h。显示出强韧化设计的有效性，为组件结构材料的进一步优化设计和长时持久强度提升奠定了基础。

关键词：一体化快堆；燃料包壳材料；铁素体/马氏体钢；辐照性能；持久强度
DOI:10. 20057/j. 1003-8620. 2024-00278　　**中图分类号：**TG142. 73

Research Progress on Ferritic/Martensitic Steels for Integrated Fast Reactor Fuel Cladding

Feng Wei[1], Guan Songyuan[2,3], Li Junhong[1], Shan Pengzhan[2,3], Xing Weiwei[2,3],
Hao Xianchao[2,3], Liang Tian[2,3], Ma Yingche[2,3]
(1 China Institute of Atomic Energy, Beijing 102413, China; 2 Shi-changxu Innovation Center for Advanced Materials, Institute of Metal Research, Chinese Academy of Sciences, Shenyang 110016, China; 3 CAS Key Laboratory of Nuclear Materials and Safety Assessment, Institute of Metal Research, Liaoning Shenyang 110016, China)

Abstract: The integrated fast reactors use metallic fuel, with fuel cladding operating at temperatures ranging from 350 ℃ to 630 ℃ and a service lifespan exceeding 50 000 hours. As the operational cycle extends, the fast neutron irradiation dose of the cladding will increase from the current 80 dpa of MOX fuel to 150 dpa-300 dpa. Therefore, the developing new cladding materials with high thermal resistance and excellent irradiation performance has become an important part of the integrated fast reactor development. This paper summarized the background of ferritic/martensitic steels (FM steels) development, analyzed the mechanical properties and irradiation performance of various FM steels, and investigated the influence of different alloying elements on these properties. Based on these analyses, alloy optimization strategies for FM steels suitable for integrated fast reactor fuel cladding were proposed. The optimization strategy was initially modified for HT9 steel, and the modified HT9G was tested for room temperature tensile test and 700 ℃/100 MPa creep rupture life. The results show that the modified alloy exhibits excellent tensile strength and creep rupture life, its room temperature yield strength reaches 880 MPa, which is approximately 310 MPa higher than that of T91 steel and 80 MPa-120 MPa higher than that of HT9 and T92 steels. Under conditions of 700 ℃ and 100 MPa, the creep rupture life is 372 hours-385 hours, significantly exceeding the 70 hours-82 hours of HT9 under the same conditions. It shows the effectiveness of toughening design, laying the foundation for further optimization of component structural materials and enhancement of long-term durability and strength improvement.

Key Words: Integrated Fast Reactor; Fuel cladding; Ferritic/martensitic steel; Irradiation performance; Creep property

一体化闭式循环快堆核能系统（以下简称“一体化快堆”）是在同一地址建设快堆、干法后处理厂和燃料生产线，通过高质量闭式燃料循环，实现铀资源的高效利用和废物最小化是我国核能“三步走”战略的重要一环[1]。一体化快堆的建设基于钠冷快堆[2]，但与钠冷快堆相比，一体化快堆燃料形

基金项目：中国科学院战略性先导科技专项(XDA0410000)
作者简介：冯 伟（1987—），男，博士，高级工程师；　**E-mail：**fengwei1109@sina.com；
收稿日期：2024-12-15
通信作者：马颖澈（1976—），男，博士，研究员；　**E-mail：**ycma@imr.ac.cn

式、换料周期、燃耗等发生明显变化。一体化快堆采用金属合金燃料，其燃料燃耗由快堆的10at.%[3]（at.%为燃耗单位，指核燃料中裂变的原子数占总重金属原子数百分比）提高至15~20at.%[4]，燃料工作周期由近20 000 h增至50 000 h以上，相应地堆芯材料所承受的辐照剂量由80dpa增加至150~300 dpa。燃料包壳是燃料组件中服役环境最为苛刻的部件，不仅承受高辐照剂量，其工作温度和寿期末承受的应力分别达到600~630 ℃ ℃和35~55 MPa。“长寿命、深燃耗、高应力”的服役工况对包壳材料的耐辐照性、高温长时力学性能及组织稳定性都提出了更高的要求。

奥氏体耐热钢[5-6]、9%~12%Cr铁素体/马氏体耐热钢（以下简称“FM钢”）[7-8]和纳米氧化物强化的铁素体或铁素体/马氏体钢（以下简称“ODS钢”）[9-10]是一体化快堆包壳材料的主要候选材料。15Cr-15Ni体系奥氏体耐热钢是钠冷快堆包壳材料的主要候选材料，承温能力可以达到650~700 ℃，其不足之处在于快中子辐照剂量达到80~100 dpa后易于发生肿胀，严重时可能引起包壳破裂[5-6, 11]。ODS钢具有良好的高温强度和抗辐照肿胀性能，被认为是一体化块堆长远发展的包壳候选材料。该材料目前研究主要集中在材料体系的发展[9-10, 12-14]，中试或近工程化级别的制备技术研究等方面[15]。FM钢具有良好的工程制造和应用经验，抗辐照肿胀性能得到验证[16-17]，是一体化快堆包壳材料极具潜力的候选材料，其主要不足在于高温强度偏低而使得承温能力通常限制在620 ℃以下[17]。自1980年代以来，世界范围内针对核用FM钢的研发取得了长足进步，提出了系列强韧化技术手段，使得FM钢的承温能力由早期HT9钢的550~580 ℃提升到T92钢的600~620 ℃[18]。尽管新近发展的SAVE12AD钢[19]、MARBEN[20]和G115[21]使用温度达到了630~650 ℃，然而其采用的w[Co]3%、w[B]0.015%合金化策略不适宜于核能应用。因此，突破核用FM钢强韧化技术瓶颈，发展承温能力满足高燃耗燃料包壳发展需求的FM钢，成为我国一体化快堆技术发展的重要部分。

本文简要回顾了FM钢发展历史，汇总分析了系列FM钢性能以及关键合金元素对FM钢性能的影响，提出了提升HT9钢承温能力的强韧化策略。对现有实验研究结果进行了汇总，验证了强韧化的有效性，显示出改进型FM钢满足一体化快堆包壳应用的强度需求，具备高温应用的前景。

1 FM钢发展及其在钠冷快堆中的应用

FM钢的发展起源于火电站热效率提升的技术需求，促进了火电机组实现了亚临界向超临界、超超临界的跨越[21]。按照600 ℃、10万小时持久强度进行划分，火电用FM钢主要经历了5个发展阶段[22]，见表1。

核用FM钢继承了表1所示的发展脉络，并基于抗辐照性能、与冷却剂相容性、服役温度、承受的应力等的差异化而有所不同，其主要钢种及成分见表2。

20世纪70年代美国在发展钠冷快堆技术过程中选用12%Cr型HT9钢制作燃料组件（前期用于外套管和包壳管，后期包壳改用15Cr-15Ni钢），是辐照性能数据最多、研究最为全面的钢种[23]。蒸汽发生器回路选用2.25Cr-1Mo体系耐热钢，并沿用至今[24]。同时期，欧洲钠冷快堆燃料组件材料选用FV448钢、1.4914或EM10钢，并发展出了EM12钢[24]。为了解决2.25Cr-1Mo体系耐热钢在高温钠中的脱碳问题和高温强度不足的问题，美国发展的快堆蒸汽发生器改选9Cr型FM钢，发展出改进型9Cr-1Mo-V-Nb钢[25]，即在超超临界火电机组中获得广泛应用的T/P91钢。通过添加B和采用W和Mo协同强化的合金化措施，在T/P91钢基础上发展出T/P92钢[26]。日本原子能机构为满足钠冷快堆技术发展需求，开展了PNC-FM钢的研制，并应用于JSFR（Japan Sodium-cooled Fast Reactor）[27]。俄罗斯

表1 FM钢发展代系强韧化策略及代表钢种

Table1 Strengthening and toughening strategies for FM steel development generations and representative steel grades

代系	强韧化策略	600 ℃、10万小时持久强度/MPa	代表钢种
初始	采用Mo进行强化	40	T22、T9、EM10
第1代	优化Mo、添加V或Nb	60	HT9、EM12
第2代	降低C，优化Nb和V，添加N	100	T91
第3代	以W代Mo，添加B或Cu	140	T92、E911、T122
第4代	高W、B，添加Co、Cu	180	SAVE12AD、MARBEN、G115

主导的钠冷快堆燃料组件用FM钢牌号为EP450,其与美欧日材料体系和组织控制差异显著,独树一帜[28]。近期,美国泰拉能源公司提出了改型HT9钢用于支撑行波堆(钠冷快堆的一种)技术的发展[29],俄罗斯推出了EK181、ChS139和EP450-ODS钢以满足新型钠冷快堆技术发展需求[30],韩国采用优化成分的措施发展出9%Cr体系的FC92钢用于制造包壳管[31]。

为满足聚变堆和加速器驱动次临界系统(Accelerator Driven Sub-critical System, ADS)技术发展需求,低活化FM钢应运而生,先后发展出9Cr-2WVTa、F82H、JLF-1、Eurofer97、CLAM等钢种,其高温强度与T/P91钢相当,承温能力通常控制在600 ℃左右[32]。2000年以来发展的SAVE12AD、MARBEN和G115主体成分为Fe-9Cr-3 W-3Co,采用Cu、B、N、V、Nb进行复合强化[19-21],使用温度可以达到650 ℃。不足之处在于,典型钢种中的w[Co]通常高达3%,w[B]大多控制在0.01%~0.015%,添加一定量的Cu(如G115钢),在快中子辐照环境中引起嬗变反应而生成^{60}Co、He或Cu团簇,使其不适合应用在承受高辐照剂量的燃料组件上。

通过机械合金化的方法在FM钢中添加一定量的纳米Y_2O_3颗粒[30,33-34],可以有效提高其高温强度,由此发展出ODS钢满足了高承温能力的技术需求,代表牌号有ODS-Eurofer97,EP450-ODS,12YWT等。为了满足规模化应用需求,研发适用于钠冷快堆和一体化快堆包壳服役环境的材料体系、发展近工程化级别的制备技术、建立材料性能数据库(集)是ODS钢发展的主要趋势[15]。

2　FM钢典型性能

2.1　辐照性能

2.1.1　辐照肿胀

燃料组件中的包壳和外套管经受150~300 dpa剂量辐照,组织中形成孔洞而产生肿胀[35],使得组件发生一定程度的变形,严重时引起破损,对反应堆安全运行造成不利影响。FM钢抗辐照性能总体偏优,但辐照行为与钢中的Cr含量密切相关。图1[35-38]显示,随着快中子辐照剂量由100 dpa增加到200 dpa,12%Cr型的HT9钢辐照肿胀率不足1.5%,而9%Cr型T91钢的肿胀率可达到2.5%以上,即12%Cr钢在高辐照剂量条件下的抗辐照肿胀性能优于9%Cr钢。Dvoriashin A M等[39]的研究显示,在90 dpa辐照剂量下,EP-450钢最大肿胀率不超过1%。与HT9钢相比,EP-450钢表现出较大的肿胀率,这可能与该钢中较高含量δ-铁素体,促进了辐照肿胀有关。几种典型的低活化钢在多离子束辐照下的肿胀率如图2[40-41]所示。随辐照剂量的增加,均出现了低稳态膨胀向高稳态膨胀转变的过渡剂量。在多离子束辐照剂量小于40 dpa之前,JLF-1钢表现出良好抗辐照肿胀性,肿胀率仅为0.2%左右,辐照超过过渡剂量时,肿胀率迅速上升。与JLF-1相比,F82H钢过渡剂量相对较低。几种典型ODS钢的辐照肿胀行为如图3所示[7,40]。ODS-MA957与ODS-YWT钢辐照肿胀率表现出明显的辐照强度相关性,显示出良好的抗辐照肿胀性。其中,ODS-MA957在辐照剂量400 dpa时,肿胀率低于1%。

2.1.2　辐照硬化

辐照硬化表现为FMS钢辐照前后屈服强度和

表2　各代表钢种主要成分范围

Table2　The main chemical composition range of each representative steel grade

钢种	成分范围(质量分数)/%
HT9	Fe-12Cr-1Mo-0.6Mn-0.6Ni-0.52 W-038Si-0.3V-0.2C[23]
T/P9	(8~9.5)Cr-(0.85~1.05)Mo-(0.3~0.6)Mn-(0.2~0.5)Si-(0.18~0.25)V-(0.08~0.12)C-(0.06~0.1)Nb-(0.03~0.07)N-(≤0.4)Ni[25]
T/P92	(0.07~0.13)C-(≤0.05)Si-(0.3~0.6)Mn-(8.5~9.5)Cr-(≤0.4)Ni-(0.3~0.6)Mo-(0.15~0.25)V-(0.04~0.09)Nb-(1.5~2)W-(0.05~0.07)N-(0.001~0.006)B[26]
PNC-FM	(0.09~0.15)C-(0.1~0.5)Si-(0.2~0.6)Mn-(≤0.02)P-(≤0.1)S-(10.5~11.5)Cr-(0.3~0.6)Mo~(0.1~0.3)V-(0.02~0.06)Nb-(0.2~0.5)Ni-(≤0.2)Cu-(0.1~0.3)Co-(0.1~0.3)W-(0.001~0.003)B[27]
EP-450	(11~13.5)Cr-(1.2~1.8)Mo-0.8Mn-0.5Si-(0.3~0.6)Nb-(0.05~0.3)Ni-(0.1~0.3)V-(0.1~0.15)C-0.004B[28]
G115	(0.06~0.1)C-(8~9.5)Cr-(2.5~3.5)W-(2.5~3.5)Co-(0.2~0.8)Mn-(0.1~0.3)V-(0.1~0.5)Si-(0.8~1.2)Cu-(0.03~0.07)Nb-(0.006~0.01)N-(0.01~0.016)B-(≤0.03)Ni[21]
ODS-Eurofer97	(9~10)Cr-1 W-0.2V-0.1Ta-0.1C-0.2Si-(0.3~0.5)Y_2O_3[33]
EP450-ODS	13Cr-2Mo-0.12C-0.5Y_2O_3[30]
12YWT	12.3Cr-3Mo-0.4Ti-0.25Y_2O_3[34]

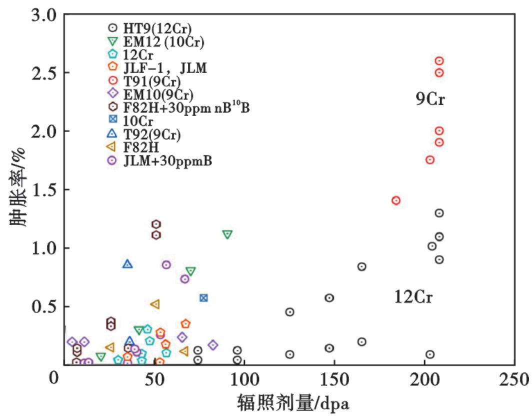

图1　快中子辐照剂量与FM钢肿胀率关系

Fig. 1　Relationship between fast neutron irradiation dose and swelling rate of FM steels

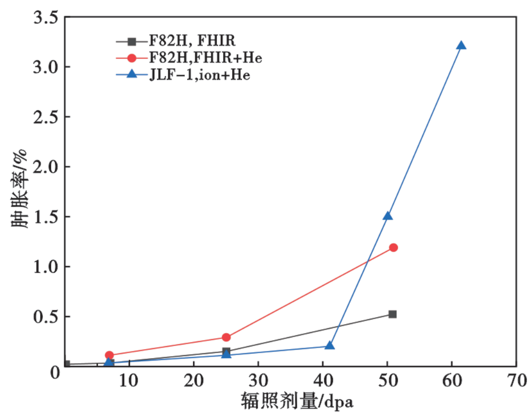

图2　多离子束辐照下辐照剂量与低活化钢肿胀率关系

Fig. 2　Relationship between irradiation dose and swelling rate of low activation steel under multi-ion beam irradiation

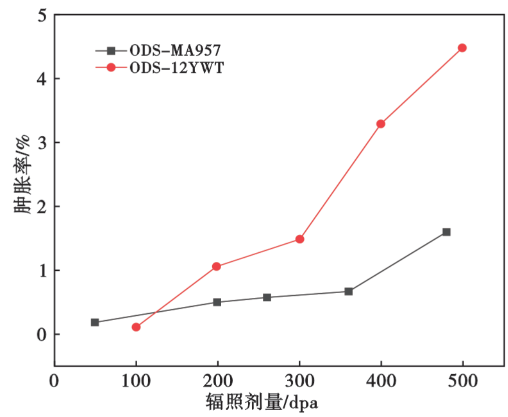

图3　快中子辐照剂量与ODS钢肿胀率关系

Fig. 3　Relationship between fast neutron irradiation dose and swelling rate of ODS steels

抗拉强度明显增大，这与辐照温度和辐照剂量密切相关。图4(a)[42]指出在300~350 ℃范围内FMS钢表现出明显的辐照硬化现象，相同辐照剂量条件下9%Cr型EM10和T91钢屈服强度增量($\Delta\sigma_y$)高于12%Cr型的HT9和PNC-FMS钢。在365 ℃辐照6.4~7.6 dpa后，T91钢的$\Delta\sigma_y$介于149~156 MPa，而HT9钢的$\Delta\sigma_y$介于345~382 MPa。在390 ℃辐照12 dpa后，T91钢的$\Delta\sigma_y$为307 MPa，而HT9钢的$\Delta\sigma_y$随热处理制度变化在125~231 MPa范围内变化。随辐照温度升高到400 ℃，不同Cr含量的FMS钢辐照硬化显著减小。图4(b)[43]显示，辐照硬化随辐照剂量增大而增大，在70~80 dpa左右变化趋于平衡。与FM钢类似，低活化钢与ODS钢均表现出明显的辐照硬化，辐照导致钢材屈服强度显著提高。图5[44-46]表明，F82H，JLF-1与EUROFER钢屈服强度增量($\Delta\sigma_y$)随辐照剂量增加，增长趋势相似。辐照剂量30~40 dpa时，辐照硬化逐渐趋于稳态，屈服强度增量均趋近于500 MPa。如图6所示[47]，ODS钢辐照条件下表现出明显的辐照硬化行为，在相同辐照温度范围内，不同种类的ODS钢屈服强度增量($\Delta\sigma_y$)随辐照强度的增加呈现出上升后趋于稳定的规律变化，辐照剂量40~50 dpa时，辐照硬化逐渐趋于稳态。

2.1.3　辐照脆化

辐照脆化表现为拉伸塑性(伸长率)降低、冲击吸收能量减小和韧脆转变温度(DBTT)升高。随着辐照硬化增加，拉伸塑性(伸长率)降低[48]。通常地，9%~12%Cr钢辐照后均发生冲击吸收能量减小和韧脆转变温度升高的现象，其中12%Cr钢变化幅度约为9%Cr钢的2倍，如图7所示[49]。关于HT9钢的研究显示，在365 ℃辐照10~17 dpa后，DBTT变化趋于饱和，如图8所示[49]。9Cr-2 W低活化钢辐照后DBTT变化幅度低于9Cr-1Mo，显示出W合金化的有益之处[50]。如图9所示[50]低活化钢表现出与FM钢类似的辐照脆化趋势，在辐照条件下，辐照剂量的上升导致韧脆转变温度(DBTT)的显著上升。EUROFER97钢相较于F82H钢，其DBTT变化趋势更快，300 ℃辐照0.3~2.4 dpa后，EUROFER97钢DBTT从7 ℃上升至78 ℃。0-5 dpa辐照后F82H钢DBTT由20 ℃上升至107 ℃。

2.2　蠕变性能

图10[51-57]汇总了9~12%Cr型FM钢蠕变性能。根据持久应力-寿命关系和热强参数方程开展了不同FM钢在600~650 ℃长时持久强度预测，结果列入表3。可以看出，在高温条件下，T92、PNC-FM和FC92钢持久强度优于HT9钢和T91钢，这是由于采用以W代Mo、通过添加N促进MX相析出或添加B

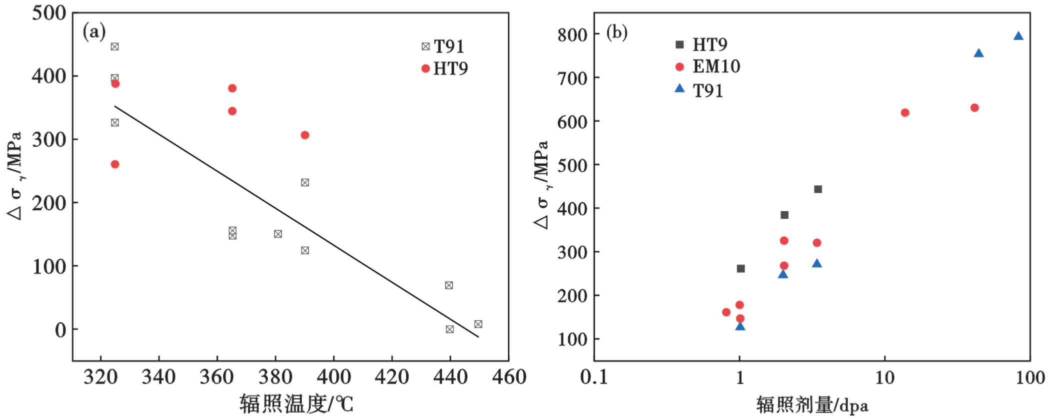

图4　9%~12%Cr钢辐照硬化行为:(a)辐照温度与$\Delta\sigma_y$关系,(b)300 ℃辐照剂量与$\Delta\sigma_y$关系

Fig. 4　Irradiation hardening behavior of 9%-12% Cr steels: (a) relationship between irradiation temperature and $\Delta\sigma_y$, (b) relationship between irradiation dose at 300 ℃ and $\Delta\sigma_y$

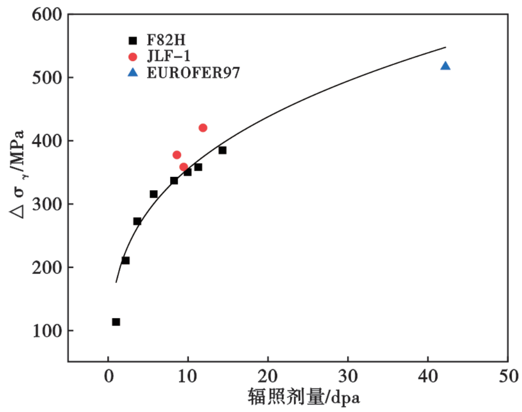

图5　低活化钢辐照硬化行为:300~325 ℃辐照剂量与$\Delta\sigma_y$关系

Fig. 5　Irradiation hardening behavior of low activation steel : (a) relationship between irradiation temperature and σ_y, (b) relationship between irradiation dose and $\Delta\sigma_y$ at 300 ℃-325 ℃

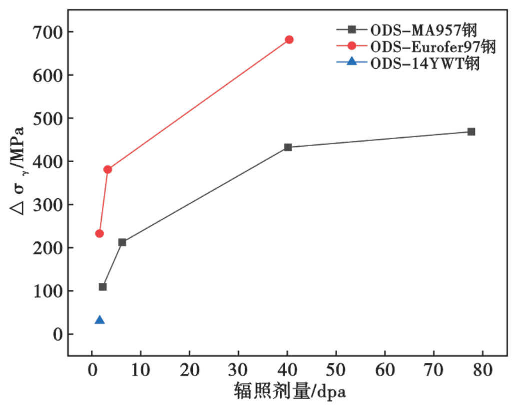

图6　ODS钢300~340 ℃辐照剂量与$\Delta\sigma_y$关系

Fig. 6　The relationship between irradiation dose and $\Delta\sigma_y$ of ODS steel at 300 ℃-340 ℃

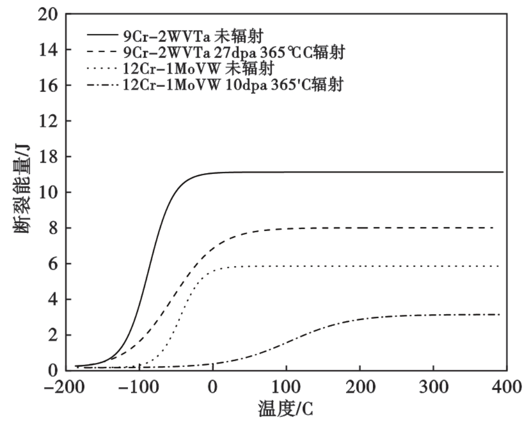

图7　365 ℃辐照对HT9(12Cr-1MoVW)和T91(9Cr-2WVTa)钢冲击性能的影响

Fig. 7　Impact of 365 ℃ irradiation on the impact toughness of HT9 (12Cr-1MoVW) and T91 (9Cr-2 WVTa) steels

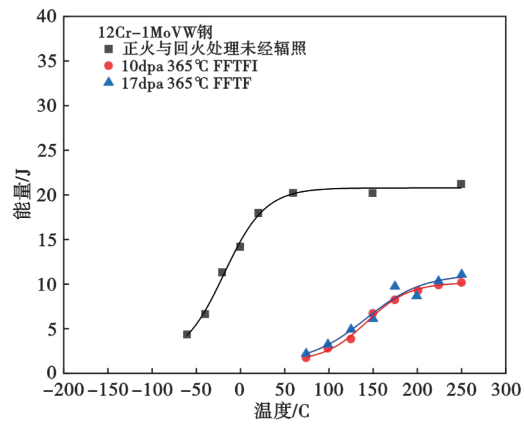

图8　辐照剂量对HT9(12Cr-1MoVW)钢冲击性能的影响

Fig. 8　Effect of irradiation dose on the impact toughness of HT9(12Cr-1MoVW) steel

的结果。通过进一步优化成分和改善合金化程度,是核用FM钢强度提升、承温能力提高的关键所在[58]。图11[40,59-60]汇总了不同ODS钢蠕变性能。其中650 ℃下ODS-12Cr钢表现出最为优异的持久强

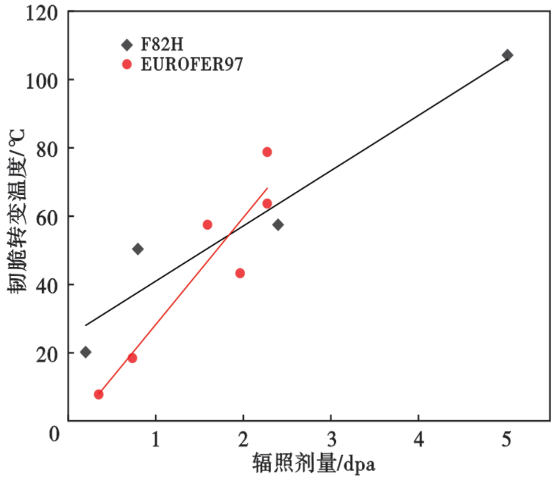

图 9　300 ℃下辐照对 F82H 与 EUROFER 钢韧脆转变温度影响

Fig. 9　Effect of irradiation at 300 ℃ on DBTT of F82H and EUROFER steels

度。这主要由于在 ODS 钢中大量弥散存在的氧化物颗粒与小角度高强度晶界[59]，使得 ODS 钢的蠕变强度普遍高于 FM 钢。

Jeong E H 等[61]的研究指出，适量添加 B 元素使 FC92 在 650 ℃、100 MPa 下的断裂时间达到 7 000 h，而不含 B 的钢蠕变断裂时间仅有 2 500 h 左右。科研人员对 EP450 的蠕变性能做了研究[62]，发现在 60 MPa 载荷，700 ℃蠕变环境下合金的蠕变断裂寿命达到 1 000 h。当处于 140 MPa，650 ℃蠕变环境下合金的蠕变速率为 $1.2\times10^{-2}\ h^{-1}$。120 MPa，700 ℃蠕变环境下，EP450 蠕变速率为 $8\times10^{-2}\ h^{-1}$。Uehira A 等[63]探究了 PNC-FM 钢的辐照蠕变状况，发现 PNC-FM 钢的抗辐照肿胀性能优异，应力引起的肿胀几乎可以忽略不计。

3　FM 钢性能退化机制及合金化策略

3.1　FM 钢性能退化机制

9%~12%Cr 型 FM 钢典型组织如图 12、图 13 所示[64]，按照介观和微观次序细分为原奥氏体晶粒（PAG）、马氏体板条、析出相和位错。高温和应力作用下，PAG 和马氏体板条界面上的碳化物易于粗化，导致其对板条、位错钉扎能力下降，板条内位错合并反应加速，促进了板条宽化和亚晶形成，是 FM 钢高温力学性能下降的主要原因[65]。如何通过合金设计优化等手段降低碳化物粗化速率，使析出相更为弥散、细小，在服役过程中可以继续有效钉扎位错，延缓亚晶形成，是提高该材料的高温持久强度，进而研发出承温能力更为优异的、适用于一体化快堆深燃耗燃料组件使用的铁马钢所首先要解决的问题。

3.2　燃料包壳用 FM 钢成分优化策略

FM 钢高温强度与板条马氏体、强化相的稳定性密切相关。Cr 是典型的铁素体形成元素，也是 $M_{23}C_6$ 形成元素，能够促进碳化物的生成[66]，过度添加会使蠕变强度降低。Cr 含量过高会导致固溶处理后形成 δ-铁素体相，并促进 FeCr 化合物析出，使强度和韧性降低[67]。在 FM 钢中，Cr 含量的增加也会增大 Z 相的析出驱动力[68]，促使 Z 相析出。Z 相为有害相，对 FM 钢力学性能产生不利影响。Cr 含量与 FM 钢的辐照行为也存在较大的关系，随着 Cr 含量的升高，铁马钢的辐照硬化程度增大[69]，但 Cr 含量升高可以提高 Cr 的扩散率，减少钢中的空位型缺陷，提高铁马钢的抗辐照肿胀性能[42]。此外，关于 FM 与高温钠液相容性研究显示，*w*[Cr]含量低于 10.5% 的钢易于发生脱碳现象[70]。

V、Nb 和 Ta 为 MX 形成元素，通过与 C 或 N 结合

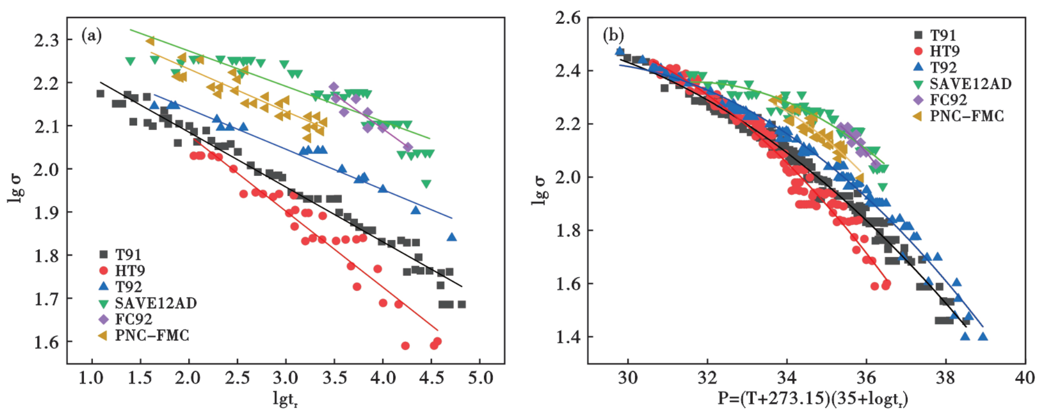

图 10　FM 钢(a)650 ℃持久应力-寿命关系曲线和(b)热强参数曲线

Fig. 10　(a) Stress-rupture life relationship curve of FM steel at 650 ℃, and (b) Larson-Miller analysis of long-term strength of FM steels

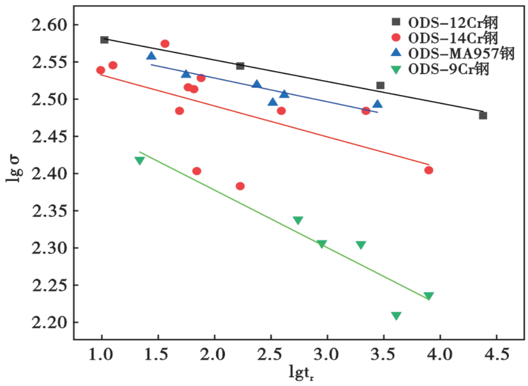

图 11　ODS 钢 650 ℃持久应力-寿命关系曲线

Fig. 11　Stress-rupture life relationship curve of FM steel at 650 ℃

表 3　不同牌号高铬铁素体/马氏体钢 600~650 ℃蠕变应力预测值

Table 3　Predicted creep stress of various grades of high-chromium FM steels at 600 ℃-650 ℃　　MPa

牌号	600 ℃/ 50 000 h	630 ℃/ 50 000 h	650 ℃/ 50 000 h	
	热强参数方程	热强参数方程	热强参数方程	持久应力-寿命关系
T91	103	72	55	55
HT9	90	56	39	40
T92	123	87	64	77
SAVE12AD	173	133	106	113
FC92	187	133	92	63
PNC-FMC	152	108	78	91

形成致密分布的碳化物和碳氮化物,对铁素体基体及晶界起到钉扎作用,加强析出相强化作用[71]。Nb 的添加,也可以增加钢的抗拉强度、屈服强度和持久强度,但会降低合金的冲击韧性[72-74]。Onizawa T 指出,在高 Cr 铁马钢中,考虑强度和塑韧性的平衡,认为 w[Nb]对钢的影响在 0.01% 时趋于饱和。作为碳化物形成元素,Nb 的添加会影响碳化物的析出,对 MX 相退化行为具有不利影响,促进 Z 相形成和粗化[72]。Ta 能够细化马氏体组织,使沉淀相均匀化[75],且 Ta 能够细化碳化物[76]。在低 C-10Cr-2Mo 钢中,w[V]和 w[Nb]的含量分别为 0.1%~0.18% 和 0.05% 时,强化效果最优[77]。Nb(C,N)主要在短时间内起析出强化作用,而 V(C,N)的析出强化作用可以延续到长时间[78]。此外,V 和 Nb,Ta 联合添加的强化作用效果更加明显,说明 V 和 Nb,Ta 组成的沉淀相是相互关联的关系[78-80]。

Mo 和 W 是促进合金固溶强化的主要元素,能够固溶进入 Fe 基体中提高蠕变强度。Mo 能够提高钢的热强性及淬透性,并且提高钢的高温强度和蠕变断裂强度[81]。W 的加入降低了 Ms 点,形成了精细的亚晶结构,减小了初始亚晶粒尺寸,延缓了 $M_{23}C_6$ 颗粒的粗化从而提高了蠕变强度[82]。将 9Cr 钢中 w[W]从 2% 提升到 3%,MC、MX 和 Z 相的粗化速率显著降低,且 W 抑制了 MX 相向 Z 相转化[83]。Abe F.[84]对比了相同 1.50Mo 当量下 W、Mo 元素对 9Cr 钢 Laves 相析出和持久强度的影响,Mo 当量的定义为 0.5 W/(0.5 W+Mo),平衡 Laves 相分数随着 W 含量的提升而增大,持久强度则随着 W 含量的提高而增强,认为 W 元素的添加相比于 Mo 元素而育具有更好的强化效果。

C 和 N 是奥氏体的组成元素,能够抑制 δ-铁素体的形成。C 和 N 含量直接影响 FM 钢中碳化物和碳氮化物的析出与粗化,随着 C 含量减少和 N 含量增加,MX 碳氮化物显著增多[85]。9%~12%Cr 钢中 w[C]应控制在 0.08%~0.16% 或 0.09%~0.14% 之间效果较好[86]。N 是提高 9%Cr 耐热钢的必需元素,其主要作用是与 V、Nb 生成 MX 相,更好钉扎晶界,从而提高高温强度和蠕变性能。N 含量过高时,会导致

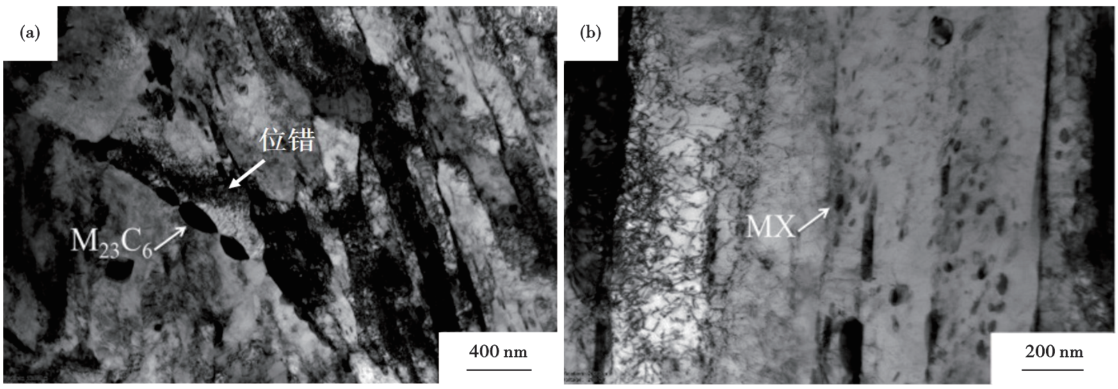

图 12　HT9 钢热处理后的显微组织:(a)位错,(b)析出相

Fig. 12　Microstructure of HT9 steel after heat treatment: (a) dislocation, (b) precipitated phase

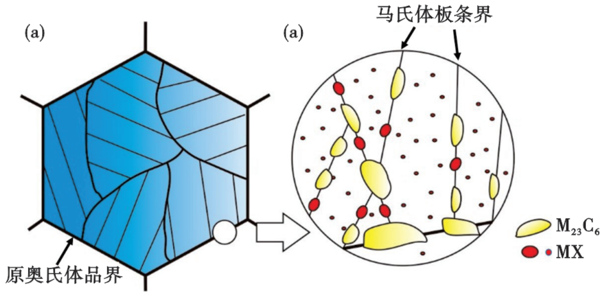

图13　HT9钢热处理后马氏体精细结构示意图：(a)奥氏体晶粒，(b)马氏体板条和$M_{23}C_6$

Fig. 13　Martensitic fine structure schematic of HT9 steel after heat treatment：(a) austenitic grains，(b) martensitic slats and $M_{23}C_6$

蠕变阶段Z相的生成[87]，Z相析出时尺寸较大，同时析出伴随着MX相的消耗，从而降低了MX相弥散强化的效果，但不会促进沉淀强化，且使9%~12%Cr铁素体耐热钢的蠕变寿命下降，对蠕变性能产生不利影响，所以应避免N含量过高生成Z相。

B属于间隙固溶元素，特别适合在晶界处的空位中存在，稳定晶界提高晶界强度。B能够明显提高12%Cr钢在650~750 ℃时的蠕变断裂强度，而当w[B]超过0.1%时，蠕变强度反而下降[88-90]。Hättestrand等指出，B会在晶界处偏析，而且主要聚集在$M_{23}C_6$沉淀相中，能提高$M_{23}C_6$相的稳定性，降低其粗化的速率[91-92]。B扩散到$M_{23}C_6$/基体界面，阻碍元素扩散，降低碳化物粗化速率，从而提高材料的强度[93]。蠕变过程中，B抑制$M_{23}C_6$相颗粒粗化而延缓板条宽化，同时促进细小MX析出[94]，提高了长期蠕变强度。Abe F.[94]通过对不同N含量FM钢的研究发现，B与N生成了粗大的BN化合物，降低高温持久强度。因此，在不生成BN的条件下，B含量越高对持久性能越有利。

3.3　新型HT9G钢研制及长时性能预测

基于元素作用的理论分析，通过添加Nb、Ta促进MX相析出，调节W/Mo和B/N比等手段，发展出成分改性的HT9钢(以下简称"HT9G钢")。

真空感应熔炼HT9G钢锭，经锻造和轧制加工成板材，经1 100 ℃正火30 min+720 ℃回火90 min后开展拉伸和持久寿命测试，结果如图14和图15所示。从图14可以看出，HT9G钢的室温屈服强度与抗拉强度显著高于HT9、T91和T92钢。其屈服强度可达880 MPa，比T91钢提高约310 MPa，比HT9和T92钢提高约80~120 MPa。抗拉强度也高于上述三种核用FM钢，达到1 046 MPa。由图15可知，HT9钢在700 ℃、100 MPa条件下的持久断裂时间仅为70~82 h，而HT9G钢持久断裂时间延长到372~385 h，持久寿命得到明显提升，显示出成分优化的有效性，为后续长时持久强度测试奠定了基础。

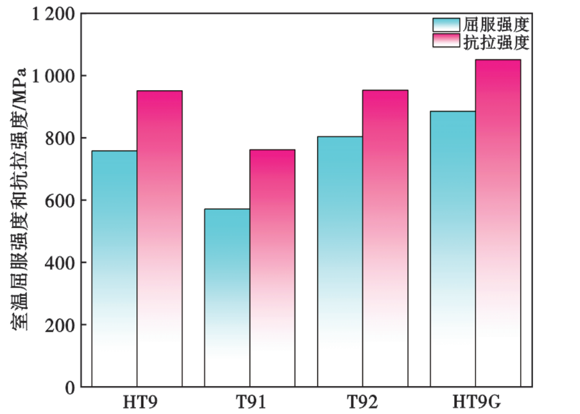

图14　HT9G合金室温拉伸性能及与HT9、T91和T92合金性能比对

Fig. 14　Comparison of room temperature tensile properties of HT9G alloy，HT9 alloy，T91 alloy，and T92 alloy

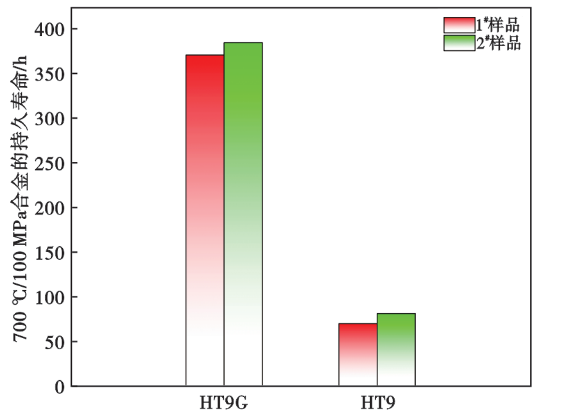

图15　HT9G合金700 ℃/100 MPa下的持久寿命及与HT9合金比对，1#样品和2#样品为同种合金的平行试样。

Fig. 15　Creep rupture life of HT9G and HT9 alloys at 700 ℃/100 MPa，Samples 1#and 2# are parallel specimens of the same alloy

4　结论

针对一体化快堆堆芯组件的材料性能要求，综述了核电体系内铁马钢牌号的发展背景以及力学性能水平。通过对铁马钢中可添加合金元素的系统分析，提出了在HT9合金的基础上，通过添加Nb相形元素，调节W/Mo比，调控适宜N、B含量，添加部分稀土元素等手段，初步优化出一种用于一体化快堆堆芯组件的改性HT9合金。该合金在室温拉伸性能测试和700 ℃/100 MPa持久寿命测试中，表现出了

远高于HT9合金的性能水平,通过后续的迭代优化,预计有望满足一体化快堆包壳材料服役指标要求。

参考文献

[1] 周培德,胡　赟,霍兴凯,等. 一体化快堆全锕系核素循环的物理可行性分析[J]. 中国核电,2024,17(4):448-453.

[2] Till C E, Chang Y I, Hannum W H. The intergral fast reactor-an overview[J]. Progress in Nuclear Energy, 1997, 31(1-2): 3-11.

[3] Ghrayeb S Z, Ivanov K N, Levine S H, et al. Burnup performance of sodium-cooled fast reactor by utilizing thorium-based fuels[J]. Nuclear Technology, 2011, 176(2): 188-194.

[4] Parrish R J, Cappia F, Aitkaliyeva A. Comparison of the radial effects of burnup on fast reactor MOX fuel microstructure and solid fission products[J]. Journal of Nuclear Materials, 2020, 531: 152003.

[5] Crawford D C, Porter D L, Hayes S L. Fuels for sodium-cooled fast reactors: US perspective[J]. Journal of Nuclear Materials, 2007, 371(1-3): 202-231.

[6] Chen S, Xie A, Lv X, et al. Tailoring microstructure of austenitic stainless steel with improved performance for generation-IV fast reactor application: a review[J]. Crystals, 2023, 13: 268.

[7] Cabet C, Dalle F, Gaganidze E, et al. Ferritic-martensitic steels for fission and fusion applications[J]. Journal of Nuclear Materials, 2019, 523: 510-537.

[8] Klueh R L, Nelson A T. Ferritic/martensitic steels for next-generation reactors[J]. Journal of Nuclear Materials, 2007, 371(1-3): 37-52.

[9] Dubuisson P, de Carlan Y, Garat V, et al. ODS Ferritic/martensitic alloys for Sodium Fast Reactor fuel pin cladding[J]. Journal of Nuclear Materials, 2012, 428: 6-12.

[10] Yang T X, Dou P. Prediction of creep rupture life of ODS steels based on machine learning[J]. Materials Today Communications, 2024, 38: 108117.

[11] Raj B, Vijiayalakshmi. Radiation damage of structural materials for fast reactor fuel assembly[J]. Joint ICTP/IAEA school on physics and technology of fast reactors systems, 2009, 2055-14.

[12] Yano Y, Tanno T, Oka H, et al. Ultra-high temperature tensile properties of ODS steel claddings under severe accident conditions[J]. Journal of Nuclear Materials, 2017, 487: 229-237.

[13] Shen J J, Li Y F, Li F, et al. Microstructural characterization and strengthening mechanisms of a 12Cr-ODS steel[J]. Materials Science and Engineering: A, 2016, 673: 624-632.

[14] Kim T K, Noh S, Kang S H, et al. Development of advanced radiation resistant ODS steel for fast reactor system applications[J]. World Journal of Engineering and Technology, 2015, 3(3): 125-128.

[15] Tanno T, Ohtsuka S, Yano Y, et al. Effects of manufacturing process on impact properties and microstructures of ODS steels[J]. Journal of Nuclear Materials, 2014, 455(1-3): 480-485.

[16] Chen Y R. Irradiation effects of HT-9 martensitic steel. Nuclear Engineering and Technology, 2013, 45: 311-322.

[17] Klueh R L. Elevated temperature ferritic and martensitic steels and their application to future nuclear reactors[J]. International Materials Reviews, 2005, 50(5): 287-310.

[18] 姜　筠,朱丽慧,王延峰. P92钢高温持久强度试验后组织变化对性能的影响[J]. 动力工程学报. 2012, 32: 898-902.

[19] Hamaguchi T, Okada H, Hirata H, et al. Creep rupture strength and microstructures of SAVE12AD welded joints[J]. Nippon steel and Sumitomo Metal Technical Report, 2018, 119: 32-38.

[20] Bhiogade D S. Ultra supercritical thermal power plant material advancements: A review[J]. Journal of Alloys and Metallurgical Systems, 2023, 3: 100024.

[21] 刘正东,陈正宗,何西扣,等. 630~700 ℃超超临界燃煤电站耐热管及其制造技术进展[J]. 金属学报,2020,56(4):539-548.

[22] Klueh R L. Ferritic/martensitic steels for advanced nuclear reactors[J]. Transactions of the Indian Institute of Metals, 2009, 62(2): 81-87.

[23] Toloczko M B, Garner F A, Eiholzer C R. Irradiation creep and swelling of the US fusion heats of HT-9 and 9Cr-1Mo to 208 dpa at ~400 ℃[J]. Journal of Nuclear Materials, 1994, 212: 604-607.

[24] Hashimoto N, Kasada R, Raj B, et al. Radiation Effects in Ferritic Steels and Advanced Ferritic-Martensitic Steels[M]. In: B. Raj, M. Vijayalakshmi eds. Comprehensive Nuclear Materials, 201, 4: 97-121.

[25] Abe F. Grade 91 heat-resistant martensitic steel[M]. In: Shibli A. eds., Coal Power Plant Materials and Life Assessment. Woodhead Publishing, 2014: 3-51.

[26] Hasegawa Y. Grade 92 creep-strength-enhanced ferritic steel[M]. In: Shibli A. eds., Coal Power Plant Materials and Life Assessment. Woodhead Publishing, 2014: 52-86.

[27] Asayama T, Nagae Y, Wakai T, et al.. International Conference on Fast Reactors and Related Fuel Cycles (FR09), 2009: 112-117.

[28] Tselishchev A V, Ageev V S, Budanov Y P, et al. Development of structural steel for fuel elements and fuel assemblies of sodium-cooled fast reactors[J]. Atomic Energy, 2010, 108(4): 274-280.

[29] Xu C, Hackett M. TerraPower HT-9 mechanical and thermal creep properties[M]. Mechanical and Creep Behavior of Advanced Materials. Cham: Springer International Publishing, 2017: 95-102.

[30] Nikitina A A, Ageev V S, Chukanov A P, et al. R&D of ferritic-martensitic steel EP450 ODS for fuel pin claddings of prospective fast reactors[J]. Journal of Nuclear Materials, 2012, 428: 117-124.

[31] Lee M, Kim G, Jung Y, et al. Radiation-induced swelling and precipitation in Fe++ ion-irradiated ferritic/martensitic steels[J]. Journal of Nuclear Materials, 2021, 555: 153137.

[32] Huang Q Y, Wang X Y, Sun S H, et al. Development of reduced activation ferritic/martensitic steels in China[J]. Journal of Nuclear Materials, 2022, 568: 153887.

[33] Lindau R, Möslang A, Rieth M, et al. Present development status of EUROFER and ODS-EUROFER for application in blanket concepts [J]. Fusion Engineering and Design, 2005, 75: 989-996.
[34] Rahmanifard R, Farhangi H, Novinrooz A J. Development of mechanical performance of 12YWT steel nanocomposite by addition of zirconium and tantalum[J]. Journal of Alloys and Compounds, 2016, 657: 646-654.
[35] Odette G R. On mechanisms controlling swelling in ferritic and martensitic alloys[J]. Journal of Nuclear Materials, 1988, 155: 921-927.
[36] Garner F A. Dimensional Stability-Swelling in Reference Module Materials Science and Materials Engineering[M]. In: Comprehensive Nuclear Materials, 2012, 4: 33-95.
[37] Klueh R L. Analysis of swelling behaviour of ferritic/martensitic steels[J]. Philosophical Magazine, 2018, 98(28): 2618-2636.
[38] Garner F A, Puigh R J. Irradiation creep and swelling of the fusion heats of PCA, HT9 and 9Cr-1Mo irradiated to high neutron fluence[J]. Journal of Nuclear Materials, 1991, 179: 577-580.
[39] Dvoriashin A M, Porollo S I, Konobeev Y V, et al. Influence of high dose neutron irradiation on microstructure of EP-450 ferritic-martensitic steel irradiated in three Russian fast reactors[J]. Journal of Nuclear Materials, 2004, 329: 319-323.
[40] Zinkle S J, Boutard J L, Hoelzer D T, et al. Development of next generation tempered and ODS reduced activation ferritic/martensitic steels for fusion energy applications [J]. Nuclear Fusion, 2017, 57(9): 092005.
[41] Ogiwara H, Sakasegawa H, Tanigawa H, et al. Void swelling in reduced activation ferritic/martensitic steels under ion-beam irradiation to high fluences[J]. Journal of nuclear materials, 2002, 307: 299-303.
[42] Klueh R L. Irradiation hardening of ferritic steels: Effect of composition[J]. Journal of Nuclear Materials, 1991, 179: 728-732.
[43] Kohno Y, Kohyama A, Hirose T, et al. Mechanical property changes of low activation ferritic/martensitic steels after neutron irradiation[J]. Journal of Nuclear Materials, 1999, 271: 145-150.
[44] Alamo A, Bertin J L, Shamardin V K, et al. Mechanical properties of 9Cr martensitic steels and ODS-FeCr alloys after neutron irradiation at 325 ℃ up to 42dpa[J]. Journal of Nuclear Materials, 2007, 367: 54-59.
[45] Luzginova N V, Nolles H S, Ten Pierick P, et al. Irradiation response of ODS Eurofer97 steel[J]. Journal of nuclear materials, 2012, 428(1-3): 192-196.
[46] Toloczko M B, Garner F A, Voyevodin V N, et al. Ion-induced swelling of ODS ferritic alloy MA957 tubing to 500dpa[J]. Journal of Nuclear Materials, 2014, 453(1-3): 323-333.
[47] Bhattacharya A, Zinkle S J, Henry J, et al. Irradiation damage concurrent challenges with RAFM and ODS steels for fusion reactor first-wall/blanket: A review[J]. Journal of Physics: Energy, 2022, 4(3): 034003.
[48] Klueh R L, Shiba K, Sokolov M A. Embrittlement of irradiated ferritic/martensitic steels in the absence of irradiation hardening [J]. Journal of Nuclear Materials, 2008, 377(3): 427-437.
[49] R. L. Klueh, D. J. Alexander. In: R. E. Stoller, A. S. Kumar, D. S. Gelles (Eds.), Effects of Radiation on Materials: 15 th International Symposium, ASTM STP 1125, American Society for Testing and Materials, Philadelphia ,1992:1256.
[50] Lucon E, Chaouadi R, Decréton M. Mechanical properties of the European reference RAFM steel (EUROFER97) before and after irradiation at 300 ℃[J]. Journal of Nuclear Materials, 2004, 329: 1078-1082.
[51] Odette G R, He M Y, Yamamoto T. On the relation between irradiation induced changes in the master curve reference temperature shift and changes in strain hardened flow stress[J]. Journal of Nuclear Materials, 2007, 367: 561-567.
[52] Kim W G, Park J Y, Choudhary B K, et al. Influence of data size on the reliability assessment of creep life of grade 91 steel[J]. Journal of Mechanical Science and Technology, 2014, 28(11): 4493-4501.
[53] 侍克献，张作贵，田根起，等. 国产主蒸汽管道用P92钢的持久性能研究[J]. 动力工程学报，2023，43(10)：1260-1267.
[54] Kim S H, Kim J H, Park S G, et al. Fabrication and Evaluation of Advanced Cladding Tube for PGSFR[J]. 2018.
[55] Lee C B, Cheon J S, Kim S H, et al. Metal fuel development and verification for prototype generation IV sodium-cooled fast reactor [J]. Nuclear Engineering and Technology, 2016, 48(5): 1096-1108.
[56] Li S, Eliniyaz Z, Zhang L, et al. Microstructural evolution of delta ferrite in SAVE12 steel under heat treatment and short-term creep[J]. Materials characterization, 2012, 73: 144-152.
[57] Steckmeyer A, Rodrigo V H, Gentzbittel J M, et al. Tensile anisotropy and creep properties of a Fe-14CrWTi ODS ferritic steel [J]. Journal of nuclear materials, 2012, 426(1-3): 182-188.
[58] Klueh R L, Shingledecker J P, Swindeman R W, et al. Oxide dispersion-strengthened steels: A comparison of some commercial and experimental alloys[J]. Journal of Nuclear Materials, 2005, 341(2-3): 103-114.
[59] Xu C. Creep rupture analysis of candidate steels for the traveling wave reactor[C]. ASME 2018 Symposium on Elevated Temperature Application of Materials for Fossil, Nuclear, and Petrochemical Industries, 2018
[60] Kim D H, Lee C M, Kim J H, et al. Thermal creep analysis and correlation development for manufactured HT9 cladding[J]. Journal of Nuclear Materials, 2024, 593: 154999.
[61] Jeong E H, Kim J H, Kim S H, et al. Creep rupture characteristics of cladding tubes of FC92B and FC92N: Candidate alloys of SFR fuel cladding tube materials[J]. Metals and Materials International, 2022, 28(6): 1445-1454.
[62] AGEEV V S, TSELISHCHEV A V, SHKABURA I A, et al. Structural materials for Russian fast reactor cores Status and prospects [R]. International Atomic Energy Agency (IAEA), 2009.
[63] Uehira A, Mizuta S, Ukai S, et al. Irradiation creep of 11Cr-0. 5Mo-2 W, V, Nb ferritic-martensitic, modified 316, and 15Cr-20Ni austenitic S. S. irradiated in FFTF to 103-206 dpa[J]. Jour-

nal of Nuclear Materials, 2000, 283: 396-399.

[64] Cerjak H, Hofer P, Schaffernak B. The influence of microstructural aspects on the service behaviour of advanced power plant steels[J]. ISIJ International, 1999, 39(9): 874-888.

[65] Ghassemi Armaki H, Chen R P, Kano S, et al. Microstructural degradation mechanisms during creep in strength enhanced high Cr ferritic steels and their evaluation by hardness measurement [J]. Journal of Nuclear Materials, 2011, 416(3): 273-279.

[66] 美) C. E. 蒂　尔(Charles E. Till), (美)张润一(Yoon IL Chang)著【★】霍兴凯. 无尽的能源:一体化快堆[M]. 北京:中国原子能出版社, 2020: 93-108.

[67] 王　晨. 合金元素及热处理工艺对ZG1Cr_{10}MoNiVNbN钢的组织和性能的影响[D]. 哈尔滨:哈尔滨理工大学, 2017.

[68] 张二红, 张华龙. 马氏体不锈钢发展现状与趋势[J]. 煤矿机械, 2014, 35(12): 16-18.

[69] Golpayegani A, Andrén H O, Danielsen H, et al. A study on Z-phase nucleation in martensitic chromium steels[J]. Materials Science and Engineering: A, 2008, 489(1-2): 310-318.

[70] Chiapetto M, Malerba L, Becquart C S. Effect of Cr content on the nanostructural evolution of irradiated ferritic/martensitic alloys: An object kinetic Monte Carlo model[J]. Journal of Nuclear Materials, 2015, 465: 326-336.

[71] Shikakura S, Nomura S, Ukai S, et al. Development of high-strength ferritic/martensitic steel for FBR core materials[J]. Journal of the Atomic Energy Society of Japan, 1991, 33(12): 1157-1170.

[72] Abe F, Taneike M, Sawada K. Alloy design of creep resistant 9Cr steel using a dispersion of nano-sized carbonitrides[J]. International Journal of Pressure Vessels and Piping, 2007, 84(1-2): 3-12.

[73] 姚　斌. Nb含量对2$Cr_{11}Mo_1$VNbN耐热钢的组织和性能的影响[J]. 特钢技术, 2019, 25(4): 6-9+18.

[74] 王哨兵, 孙文强, 王　曼, 等. Nb对GH4169合金管材组织性能的影响[J]. 特殊钢, 2024, 45(5): 34-39.

[75] Anjum M W, Wen D H, Wang Q, et al. Influence of Ta/Zr minor-alloying on the high-temperature microstructural stability of cladding Fe-Cr-Al ferritic stainless steels[J]. Journal of Nuclear Materials, 2019, 522: 19-31.

[76] Zhang S Q, Li J C, Peng Z X, et al. Synergistic effects of Ta and Mo on the hydrogen embrittlement resistance in ultra-high strength hot stamping steel[J]. Materials Science and Engineering: A, 2023, 872: 144956.

[77] Kim H K, Lee J W, Moon J, et al. Effects of Ti and Ta addition on microstructure stability and tensile properties of reduced activation ferritic/martensitic steel for nuclear fusion reactors[J]. Journal of Nuclear Materials, 2018, 500: 327-336.

[78] Sanhueza J P, Rojas D, Prat O, et al. Investigation of Ta-MX/Z-phase and laves phase as precipitation hardening particles in a 12Pct Cr heat-resistant steel[J]. Metallurgical and Materials Transactions A, 2018, 49(7): 2951-2962.

[79] Fujita T, Asakura K, Sawada T, et al. Creep rupture strength and microstructure of low C-10Cr-2Mo heat-resisting steels with V and Nb[J]. Metallurgical Transactions A, 1981, 12(6): 1071-1079.

[80] Lee K H, Hong S M, Shim J H, et al. Effect of Nb addition on Z-phase formation and creep strength in high-Cr martensitic heat-resistant steels [J]. Materials Characterization, 2015, 102: 79-84.

[81] Grobner P J, Hagel W C. The effect of molybdenum on high-temperature properties of 9 pct Cr steels[J]. Metallurgical Transactions A, 1980, 11(4): 633-642.

[82] Abe F, Nakazawa S. The effect of tungsten on creep[J]. Metallurgical Transactions A, 1992, 23(11): 3025-3034.

[83] Fedoseeva A, Dudova N, Kaibyshev R, et al. Effect of tungsten on creep behavior of 9%Cr-3%Co martensitic steels[J]. Metals, 2017, 7(12): 573.

[84] Abe F. Progress in creep-resistant steels for high efficiency coal-fired power plants[J]. Journal of Pressure Vessel Technology, 2016, 138(4): 040804.

[85] 殷凤仕, 刘志良, 薛　冰, 等. 微量碳和氮对9%Cr耐热钢中第二相析出行为的影响[J]. 动力工程学报, 2010, 30(4): 258-262.

[86] 朱　麟. 高铬耐热钢高温蠕变行为及寿命预测[D]. 西安:西北大学, 2019.

[87] Sawada K, Taneike M, Kimura K, et al. Effect of nitrogen content on microstructural aspects and creep behavior in extremely low carbon 9Cr heat-resistant steel[J]. ISIJ International, 2004, 44(7): 1243-1249.

[88] Hättestrand M, Andrén H O. Boron distribution in 9-12% chromium steels[J]. Materials Science and Engineering: A, 1999, 270(1): 33-37.

[89] El-Kashif E, Asakura K, Shibata K. Effects of nitrogen in 9Cr-3W-3Co ferritic heat resistant steels containing boron[J]. ISIJ International, 2002, 42(12): 1468-1476.

[90] Jeong E H, Kim J H, Kim S H, et al. Influence of B and N on the microstructural characteristics and high-temperature strength of 9Cr-2 W steel during an aging treatment[J]. Materials Science and Engineering: A, 2017, 700: 701-706.

[91] Dudova N. 9-12% Cr heat-resistant martensitic steels with increased boron and decreased nitrogen contents [J]. Metals, 2022, 12(7): 1119.

[92] Heo H M, Jeong E H, Kim S H, et al. Comparison between effect of B and N on the microstructure of modified 9Cr-2 W steel during aging and creep[J]. Materials Science and Engineering: A, 2016, 670: 106-111.

[93] Rejeesh R, Bhattacharya A, Haldar C, et al. Relative effect of B and N concentrations on the microstructural stability and mechanical properties of modified 9Cr-1Mo steel[J]. Journal of Alloys and Compounds, 2021, 867: 158971.

[94] Abe F. Analysis of creep rates of tempered martensitic 9%Cr steel based on microstructure evolution[J]. Materials Science and Engineering: A, 2009, 510: 64-69.